

decreases is expected to be a general feature which would remain in any improved calculation.

Figure 3 shows plots of the IMFP's both with and without the effect of exchange scattering, and the change in the IMFP due to exchange. The curves for Fe, Co, and Ni all lie within about 4% of each other and we display one representative set of curves. The exchange interference term remains about a 10% effect out to 200 eV above the Fermi energy. This occurs because, although the statistical method gives highest weight to the outer region of the Wigner-Seitz cell where electron densities are lowest, the density of this region corresponds in Fe, Co, and Ni to free-electron gases with  $1.0 \leq r_s \leq 1.7$ , where  $(r_s a_0)^3 = 3/4\pi n(r)$ .

<sup>1</sup>R. E. DeWames and L. A. Vredevoe, Phys. Rev. Lett. **23**, 123 (1969).

<sup>2</sup>A. Bringer, M. Campagna, R. Feder, W. Gudat, E. Kisker, and E. Kuhlmann, Phys. Rev. Lett. **42**, 1705 (1979).

<sup>3</sup>R. Feder, Solid State Commun. **31**, 821 (1979).

<sup>4</sup>M. Campagna, private communication.

<sup>5</sup>R. J. Celotta, D. T. Pierce, G. C. Wang, G. D. Bader, and G. P. Felcher, Phys. Rev. Lett. **43**, 728 (1979).

<sup>6</sup>J. Lindhard and M. Scharff, K. Dan. Vidensk. Selsk., Mat.-Fys. Medd. **27**, No. 15 (1953); J. Lindhard, M. Scharff, and H. E. Schiff, K. Dan. Vidensk. Selsk., Mat.-Fys. Medd. **33**, No. 14 (1963).

<sup>7</sup>C. J. Tung, J. C. Ashley, and R. H. Ritchie, Surf. Sci. **81**, 409 (1979).

<sup>8</sup>R. H. Ritchie and J. C. Ashley, J. Phys. Chem. Solids **26**, 1689 (1965).

<sup>9</sup>J. Lindhard, K. Dan. Vidensk. Selsk., Mat.-Fys. Medd. **28**, No. 8 (1954).

<sup>10</sup>J. J. Quinn and R. A. Ferrell, Phys. Rev. **112**, 812 (1958).

<sup>11</sup>V. L. Moruzzi, J. F. Janak, and A. R. Williams, *Calculated Electronic Properties of Metals* (Pergamon, New York, 1978).

## Oscillatory Magnetic Fluctuations near the Superconductor-to-Ferromagnet Transition in $\text{ErRh}_4\text{B}_4$

D. E. Moncton, D. B. McWhan, and P. H. Schmidt  
*Bell Laboratories, Murray Hill, New Jersey 07974*

and

G. Shirane and W. Thomlinson  
*Brookhaven National Laboratory, Upton, New York 11973*

and

M. B. Maple, H. B. MacKay, L. D. Woolf, Z. Fisk, and D. C. Johnston  
*Institute for Pure and Applied Physical Sciences, University of California, San Diego, La Jolla, California 92093*  
(Received 26 June 1980)

Small-angle neutron experiments show that near the transition from superconductor to ferromagnet in  $\text{ErRh}_4\text{B}_4$  scattering peaks occur at a wave vector  $|\vec{q}_s| = 0.06 \text{ \AA}^{-1}$ . The temperature and wave-vector dependence suggest this signal is due to oscillatory magnetization fluctuations caused by the electromagnetic coupling of magnetic and superconducting order parameters. The ferromagnetic Bragg scattering shows a 5% hysteresis and transition-temperature-smearing effects which are also due to magnetic-superconducting interactions.

PACS numbers: 74.70.Lp, 75.25.+z

Superconductivity can develop in systems with large concentrations of magnetic ions if there is a weak interaction between the magnetic moments and the superconducting electrons. Furthermore, if the magnetic ions occupy an ordered lattice as in the rare-earth (RE) ternary superconductors  $M\text{Mo}_6X_8$  ( $M = \text{Re}; X = \text{S, Se}$ ) (Ref. 1) and  $M\text{Rh}_4\text{B}_4$  (Ref. 2) magnetic order may occur.<sup>3</sup> For antifer-

romagnetic order, superconductivity can be preserved. However, in the two known ferromagnetic superconductors,  $\text{ErRh}_4\text{B}_4$  (Ref. 4) and  $\text{HoMo}_6\text{S}_8$  (Ref. 5), the materials lose their superconductivity at a second lower-temperature transition.<sup>6,7</sup> To better understand the interaction between superconducting and magnetic order, we undertook new neutron scattering measurements on  $\text{ErRh}_4\text{B}_4$

focusing on the magnetic fluctuation effects and the ferromagnetic Bragg scattering.

In a previous study<sup>4</sup> of an  $\text{ErRh}_4\text{B}_4$  sample which becomes superconducting below  $T_{c1} = 8.5$  K, magnetic Bragg scattering developed continuously below the reentrant transition at  $T_{c2} \approx 1.0$  K. However, unusually large precursive scattering was noted due either to fluctuation effects or smearing of the transition. In this Letter, results on larger, higher-quality specimens reveal new aspects of the superconducting ferromagnetic transition due to the coupling between the two ordering phenomena. The most remarkable of these interaction effects is the suppression of the long-wavelength magnetic fluctuations as  $T_{c2}$  is approached within the superconducting phase. The resulting magnetic response peaks at a finite wave vector  $|\vec{q}_s| = 0.06 \text{ \AA}^{-1}$ .

Our neutron scattering experiments employed triple-axis spectrometers at the Brookhaven National Laboratory high-flux beam reactor with incident neutron energies of both 5 and 13.8 meV. Two specimens which contained the <sup>11</sup>B isotope were studied. Sample I was prepared by arc melting and sliced into six 1-mm-thick slabs each about  $0.5 \times 0.5 \text{ cm}^2$  in area. No annealing was performed on this sample. Its upper superconducting temperature was  $T_{c1} = 8.45$  K and its reentrant temperature was  $T_{c2} = 0.72$  K. Sample II was also prepared by arc melting and then crushed into a fine powder and annealed. Its transition temperatures were  $T_{c1} = 8.7$  K and  $T_{c2} = 0.93$  K.

This Letter focuses on the behavior of the small-angle neutron scattering which is displayed in Fig. 1. These data were obtained on sample I as it was cooled through the reentrant transition. A peak is clearly evident at  $2\theta = 1.4^\circ$  corresponding to a lattice spacing  $d = 100 \text{ \AA}$ . In the preparation of these data, we have subtracted a 4-K profile because of the main beam. As observed in both ferroelectric<sup>8</sup> and ferromagnetic<sup>9</sup> transitions, domain walls may produce additional scattering proportional to the square of the order parameter. Although we cannot prove that this is the origin of a remaining contribution at 0.07 K, we have also subtracted it (scaled by the square of the order parameter) from the data in Fig. 1. Since both of these corrections involve subtracting profiles which vary smoothly with  $2\theta$ , they do not alter the fundamental conclusion that there is yet another scattering component (that shown in Fig. 1) which peaks at a finite scattering angle and exists only over a limited temperature range

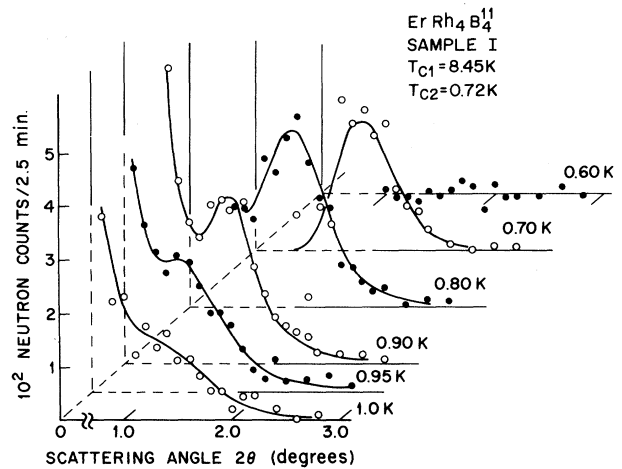


FIG. 1. Small-angle neutron-scattering results on  $\text{ErRh}_4\text{B}_4$  obtained at various temperatures with incident neutron energy of 13.8 meV. The peaks at  $2\theta = 1.4^\circ$  indicate an oscillatory magnetization with a wavelength of  $\sim 100 \text{ \AA}$ .

from about 1.1 to 0.65 K. Although these data have been available for some time,<sup>10</sup> they do not, by themselves, prove that the small-angle signal originates in the superconducting fraction of the sample. The crucial part of the present work described below enables us to firmly establish this conclusion.

Further studies involved sample II whose properties were better characterized. Figure 2 shows the temperature dependence of the magnetic part of the (101) Bragg intensity, and the specific heat measured on the identical sample. The sharp specific-heat spike at  $T_{c2} = 0.93$  K signals the bulk transition to the superconducting state on warming from the normal ferromagnetic state. At this temperature the magnetization is about 70% of its saturation value (magnetic intensity is about 50%) and no discontinuity is observable within 2%. The magnetic scattering above  $T_{c2}$  is *not* due to fluctuations, since even the weak signal at  $T = 1.4$  K has the sharp Bragg profile because of long-range order. This effective smearing of the transition is not due to chemical impurities since a similarly prepared sample of  $\text{Ho}_{0.6}\text{Er}_{0.4}\text{Rh}_4\text{B}_4$  shows a very clean magnetic transition.<sup>11</sup> We believe that smearing is a result of the macroscopic interaction between magnetism and superconductivity. The polycrystalline nature of the sample and its magnetic anisotropy may also play a role.

Hysteretic behavior is also an important feature of the transition which is observed in other

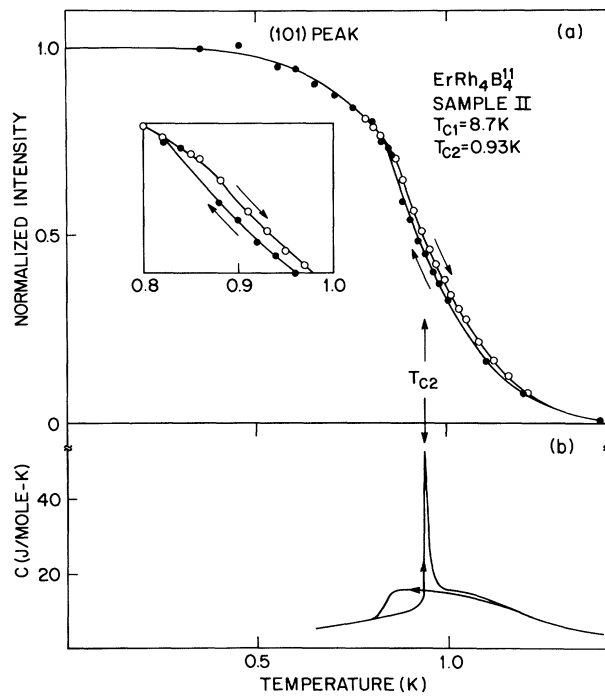


FIG. 2. Ferromagnetic Bragg intensities (a) for  $\text{ErRh}_4\text{B}_4$  are compared to specific-heat data (b) for both cooling and heating.

physical properties.<sup>12</sup> Hysteresis in the Bragg scattering persists to a temperature below  $T_{c2} = 0.93$  K [see inset to Fig. 2(a)] and has "backlash" behavior. That is, if one reverses the direction of temperature change within the loop, the signal remains nearly constant until the other curve is reached. The temperature interval over which there is hysteresis in the heat-capacity data of Fig. 2(b) ( $\sim 0.8$  K to  $\approx 1.1$  K) is in reasonable agreement with that observed in the Bragg scattering data. We speculate that the hysteresis loop defines that temperature regime over which both superconducting and ferromagnetic regions coexist in the sample.

Although the origin of hysteresis is unclear, we use it to demonstrate that the small-angle scattering shown in Fig. 1 is distinct in its origin from that of the developing ferromagnetism. In Fig. 3 the hysteresis of the small-angle scattering in sample II is shown (no background subtractions have been made). It is complementary to that of the ferromagnetic Bragg intensity in that it is greater on cooling than it is at the same temperature on heating. This observation demonstrates that the sample contains both superconducting regions with finite-wave-vector magnetic fluctuations and ferromagnetic regions which pro-

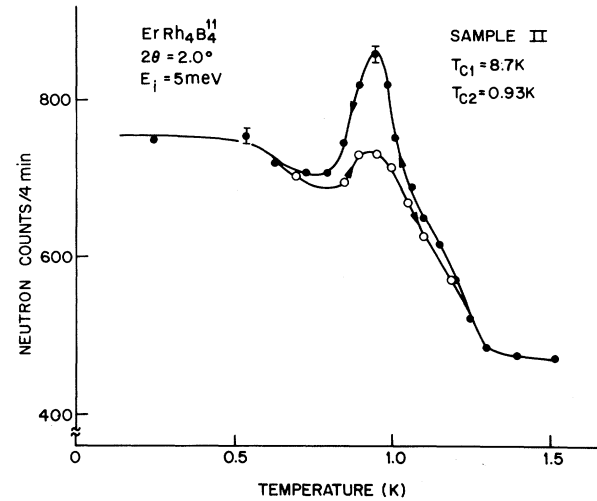


FIG. 3. The temperature dependence of the small-angle scattering signals. Substantial hysteresis is observed which is in the opposite sense of that for the Bragg scattering of Fig. 2(a).

duce normal Bragg scattering.

We briefly discuss the origin of the small-angle scattering signal. In general, in magnetic superconductors there are two important interactions. One is the exchange interaction between the rare-earth magnetic moments and the conduction-electron spins which causes both spin-flip scattering and conduction-electron polarization. The other interaction is associated with the electromagnetic coupling of the macroscopic magnetization to the superconducting order parameter.<sup>13-16</sup> In systems with type-I superconductivity, low magnetic concentration and strong ferromagnetic exchange, the electromagnetic effects are not predominant. Such a system may prefer to order at a finite wave vector as discussed by Anderson and Suhl.<sup>17</sup> Since the present systems are strongly type-II superconductors having a concentrated magnetic lattice with weak exchange, electromagnetic interactions dominate. In this case, persistent currents screen the long-wavelength magnetization fluctuations and the susceptibility peaks at a wave vector  $|\vec{q}_s| = (\lambda_L \gamma)^{1/2}$  where  $\lambda_L$  is the London penetration depth and  $\gamma$  is the magnetic stiffness (i.e., the coefficient of  $|\nabla M|^2$  in the free energy). Although the transition to ferromagnetism must be first order, a second-order transition is possible to an oscillatory state with  $q_s = (\lambda_L \gamma)^{1/2}$  which coexists with superconductivity. We believe that this state, or fluctuations into it, first predicted by Blount and Varma<sup>13</sup> is the origin of the scattering observed in Fig. 1. The

wave vector is of the correct order of magnitude, assuming a typical penetration depth (1000 Å) and magnetic stiffness (10 Å). Furthermore, the scattering is absent when the system is completely ferromagnetic and it has a hysteretic behavior which demonstrates that it originates in the fraction of the sample which is superconducting.

The above theories have been derived under the assumption that the magnetic order coexists with a state of uniform superconductivity. Although it is possible to imagine that magnetic order develops in the form of a spontaneous vortex lattice,<sup>18,19</sup> we rule out this explanation since the observed spacing of  $\sim 100$  Å would require a spontaneous magnetic field of  $10^2$  kOe. This field is physically impossible to obtain in  $\text{ErRh}_4\text{B}_4$  since the average magnetic induction associated with the saturation magnetization of  $\text{Er}^{3+}$  is about 6.5 kOe.

We thank E. I. Blount and C. M. Varma for helpful discussions and G. W. Hull for susceptibility measurements. This work was supported in part by the U. S. Department of Energy under Contract No. DE-AC02-76CH00016, and by the U. S. Department of Energy under Contract No. EY-76-S-03-0034-PA227-3 and by the National Science Foundation under Grant No. DMR-77-08469.

<sup>1</sup>Ø. Fischer, A. Treyvaud, R. Chevrel, and M. Sergent, *Solid State Commun.* **17**, 721 (1975); R. N. Shelton, R. W. McCallum, and H. Adrian, *Phys. Lett.* **56A**, 213 (1976).

<sup>2</sup>B. T. Matthias, E. Corenzwit, J. M. Vandenberg,

and H. E. Barz, *Proc. Nat. Acad. Sci. U.S.A.* **74**, 1334 (1977); J. M. Vandenberg and B. T. Matthias, *Proc. Nat. Acad. Sci. U.S.A.* **74**, 1336 (1977).

<sup>3</sup>See D. E. Moncton, G. Shirane, and W. Thomlinson, *J. Magn. Magn. Mater.* **14**, 172 (1979), and references therein.

<sup>4</sup>D. E. Moncton, D. B. McWhan, J. Eckert, G. Shirane, and W. Thomlinson, *Phys. Rev. Lett.* **39**, 1164 (1977).

<sup>5</sup>J. W. Lynn, D. E. Moncton, W. Thomlinson, G. Shirane, and R. N. Shelton, *Solid State Commun.* **26**, 493 (1978).

<sup>6</sup>W. A. Fertig, D. C. Johnston, L. E. DeLong, R. W. McCallum, M. B. Maple, and B. T. Matthias, *Phys. Rev. Lett.* **38**, 987 (1977).

<sup>7</sup>M. Ishikawa and Ø. Fischer, *Solid State Commun.* **23**, 37 (1977).

<sup>8</sup>R. A. Cowley, J. D. Axe, and M. Iizumi, *Phys. Rev. Lett.* **36**, 806 (1976).

<sup>9</sup>J. Als-Nielsen, O. W. Dietrich, and L. Passell, *Phys. Rev. B* **14**, 4908 (1976).

<sup>10</sup>D. E. Moncton, *J. Appl. Phys.* **50**, 1880 (1979).

<sup>11</sup>H. A. Mook, W. C. Koehler, M. B. Maple, Z. Fisk, and D. C. Johnston, in *Superconductivity in d- and f-Band Metals*, edited by H. Suhl and M. B. Maple (Academic, New York, 1980), p. 427.

<sup>12</sup>W. Odoni and H. R. Ott, *Phys. Lett.* **70A**, 480 (1979).

<sup>13</sup>E. I. Blount and C. M. Varma, *Phys. Rev. Lett.* **42**, 1079 (1979).

<sup>14</sup>H. Suhl, *J. Less Common Met.* **62**, 225 (1978).

<sup>15</sup>H. Matsumoto, H. Umezawa, and M. Tachiki, *Solid State Commun.* **31**, 157 (1979).

<sup>16</sup>R. A. Ferrell, J. K. Bhattacharjee, and A. Bagchi, *Phys. Rev. Lett.* **43**, 154 (1979).

<sup>17</sup>P. W. Anderson and H. Suhl, *Phys. Rev.* **116**, 898 (1959).

<sup>18</sup>C. G. Kuper, M. Revzen, and A. Ron, *Phys. Rev. Lett.* **44**, 1545 (1980).

<sup>19</sup>M. Tachiki, H. Matsumoto, T. Koyama, and H. Umezawa, *Solid State Commun.* **34**, 19 (1980).

## Phonon-Subband Exciton Interaction in Bismuth

S. Baldwin and H. D. Drew

*Department of Physics and Astronomy, University of Maryland, College Park, Maryland 20742*

(Received 2 July 1980)

Magneto-far-infrared studies of the hole cyclotron resonance and its associated subband exciton have been made for frequencies in the vicinity of the LO frequency. Just below  $\omega_{\text{LO}}$  a resonant exciton lifetime process is observed in which the hole-pocket subband exciton decays into the electron-pocket cyclotron resonance continuum via a virtual LO phonon. The experiments also give evidence for other phonon-mediated many-body processes.

PACS numbers: 71.35.+z, 71.38.+i, 78.20.Ls

The conditions for which exciton-phonon interactions can be observed are generally such that the energy gap, and therefore the exciton energy, is large in comparison with phonon frequencies.

We are presenting here the first results on a system in which the total exciton energy is comparable to the LO phonon frequency. Such a situation can arise either for very narrow energy gap